

Phonon coupling of water monomers in a solid nitrogen matrix

L. Wu, R. Lambo,^{a)} Y. Tan, A.-W. Liu, and S.-M. Hu^{b)}

Hefei National Laboratory for Physical Science at the Microscale, University of Science and Technology of China, Hefei, Anhui 230026, China

(Received 17 January 2013; accepted 27 February 2013; published online 19 March 2013)

The infrared absorption spectra of the H₂O, HDO, and D₂O monomers isolated in solid N₂ have been recorded at various temperatures between 4 and 30 K. A study of the absorption features of the ν_1 , ν_2 , and ν_3 vibrational modes for each monomer shows their optical line shapes to be strongly temperature dependent. For all three modes, a decrease in the absorption amplitude and a proportional broadening of the linewidth was observed with increasing temperature, while the integrated absorbance remained constant. These observations were explained in terms of phonon coupling, by which high frequency intramolecular modes decay by exciting matrix phonons. Fits of the linewidth for the lowest frequency ν_2 vibrational mode to the predicted vibrational relaxation rate in a solid medium gave average phonon mode frequencies consistent with the Debye frequency for solid N₂.
© 2013 American Institute of Physics. [<http://dx.doi.org/10.1063/1.4795235>]

I. INTRODUCTION

The cryogenic hosts commonly used in the matrix isolation spectroscopy of water fall into two broad categories. The first are those such as the solid rare gases (RGs) and *p*-H₂ for which the H₂O infrared (IR) spectra contain absorption bands produced by both quasi-freely rotating and non-rotating monomers.^{1,2} The second are the molecular matrices N₂ and D₂ in which H₂O monomers do not rotate, producing spectra with near-pure vibrational bands.^{3,4} The latter matrices therefore present good systems in which to study basic matrix-molecule interactions without the complexities of ro-vibrational effects. This is particularly true of solid N₂, whose relatively high sublimation temperature makes it well-suited for characterizing the temperature dependence of this interaction.

As far as we have been able to determine, the only reported study of the temperature dependent behavior of the non-rotating water monomer has been for H₂O isolated in Kr.⁵ Analysis of this system was complicated by the presence of absorption bands due to the rotating monomer. However, it was generally observed that the intensities of the non-rotational bands decreased reversibly with temperature (*T*), approximately as $1/T$. These results were explained in terms of an intermolecular dipole interaction that suppresses rotation among closely trapped monomers at low temperature. Increased separation at high temperatures weakens this dipole interaction and allows these monomers to start to rotate, thus reducing the intensities of non-rotational bands.

This explanation encounters a number of challenges. First, there is no corresponding increase in the intensities of rotational bands with temperature. Second, the existence of non-rotating H₂O monomers in certain matrices is more likely due to anisotropy in their trapping sites² than to dipole-dipole interaction. Finally, although heating can induce trapped

molecules to diffuse, thereby separating them, this effect is not known to be reversible with temperature.

In the present work, we report on the temperature-dependent behavior of the H₂O, HDO, and D₂O monomers isolated in N₂. For each monomer, the IR absorption spectra of the ν_2 bending mode and the ν_1 symmetrical and ν_3 asymmetrical stretching modes in the range of 4–30 K have been recorded. Qualitatively similar results are observed in these systems as in that of H₂O/Kr, i.e., a decrease in the intensity of the absorption peaks with increased temperature. However, we propose an alternative theory of matrix-molecule interaction as the mechanism behind these observations. Fits of the frequencies and amplitudes of the vibrational spectra against temperature show good agreement with the curves predicted in the case of matrix-induced vibrational relaxation.⁶ The matrix-molecule interaction can then be understood as phonon coupling between the water monomer and the phonon bath of the matrix.

The remainder of this paper is organized as follows: In Secs. II and III, the experimental methods and results are presented. In Sec. IV, the theory used to explain the temperature dependence of the vibrational modes is discussed. Conclusions and perspectives are summarized in Sec. V.

II. EXPERIMENTAL

As the experimental setup was similar to those used by our group in previous experiments,⁷ only a brief description is given here. The IR absorption spectra were recorded using a Fourier-Transform (FT) spectrometer (Bruker IFS120 HR). An MCT detector was used together with a Globar light source, providing detection in the range of 500–4000 cm⁻¹ with an unapodized resolution of 0.1 cm⁻¹. To minimize absorptions due to air appearing in the spectra, the FT chamber was isolated from the sample chamber and evacuated to a pressure of 40 Pa.

^{a)}Electronic mail: lambo@mail.ustc.edu.cn

^{b)}Electronic mail: smhu@ustc.edu.cn

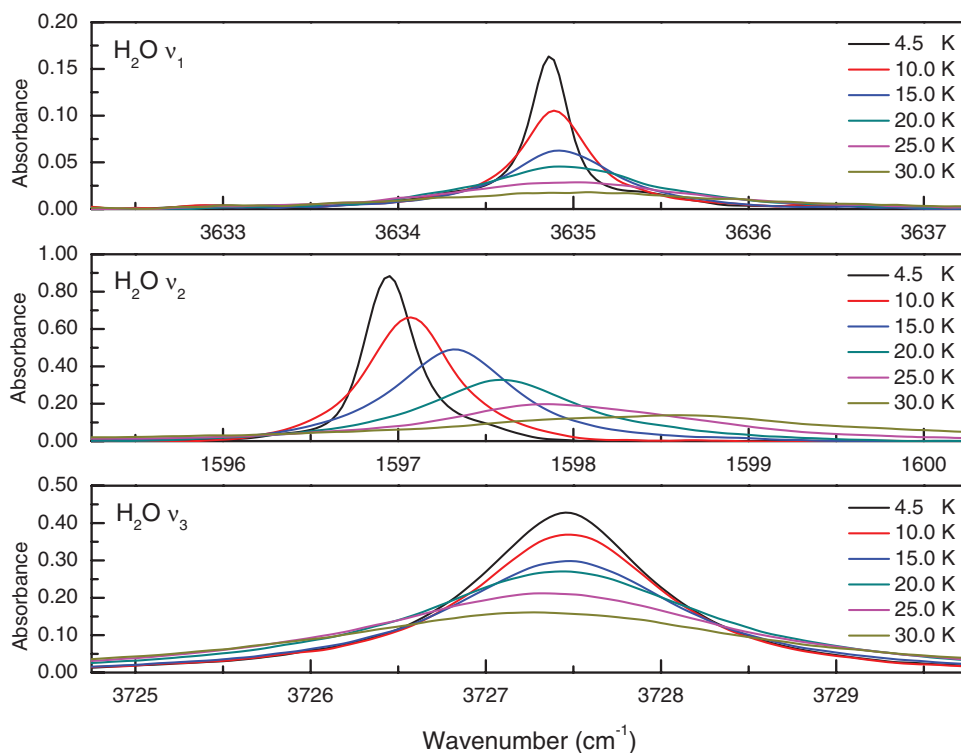


FIG. 1. Temperature dependent behavior of the H₂O ν_1 (top), ν_2 (center), and ν_3 (bottom) vibrational bands in the range of 4.5–30 K.

The matrix was grown on a 1 in. diameter BaF₂ window, selected for its optical transparency in the infrared region. It was thermally anchored to the coldhead of a closed-cycle helium refrigerator (Sumitomo-205D) in the sample chamber and evacuated to a pressure of 10^{-5} Pa. The water/nitrogen gas mixtures were produced using standard manometric techniques at a dilution of 1/2000 and deposited on the window at a flux of 5 SCCM for 1 h. Gas mixtures were prepared using N₂ ($\sim 99.9\%$ pure, Nanjing Special Gas Inc.) and, alternately, D₂O ($\sim 99.8\%$ pure, Sinopharm Chemical Reagent Co.) and triply deionized H₂O. HDO was obtained from a 1:1 mixture of liquid H₂O and D₂O, though it was not separated from these isotopologs.

Before recording the IR spectra, each matrix was first annealed by heating to 30 K over 30 min to remove any monomer occupation in thermally unstable trapping sites. A resistive heater mounted on the coldhead and controlled by a PID loop allowed us to stabilize the temperature of the BaF₂ window to within 0.2 K between 4.5 K and 30 K. The upper limit of this temperature range was determined by the fact that the structure of solid N₂ changes from that of a fcc crystal to that of a hcp crystal above 35 K. These temperatures were monitored by a silicon diode sensor (DT-470) mounted on the baseplate holding the BaF₂ window and read off a Lake Shore 331S controller.

III. RESULTS

The general features of the IR spectra of H₂O, HDO, and D₂O monomers in solid N₂ are known from previous work.^{3,8–11} In those studies, temperature effects were largely ignored and high water/nitrogen concentrations ($\sim 1/100$)

were used to generate dimers and higher aggregates together with the monomers. A much lower water/nitrogen concentration has been chosen here to suppress dimer formation, so that previously published results are not compared directly but used only as a rough guide for the assignment of the absorption peaks.

A. H₂O/N₂ absorption spectra

As can be seen in Figure 1, the most dramatic temperature effects in the H₂O/N₂ system occur for the ν_2 vibrational mode. As the temperature was increased from 4.5 K to 30 K, the amplitude of the absorption peak decreased by 84% and its linewidth broadened proportionately. There was also a simultaneous blueshift in its central frequency from 1596.0 cm^{-1} to 1598.6 cm^{-1} . Figure 1 also shows that the absorption peaks of the ν_1 and ν_3 vibrational modes underwent similar changes in the same temperature range: a decrease in their amplitudes of 87% and 61%, respectively, together with a proportional increase in their linewidths. The shifts in the central positions of these two peaks were much smaller, though a small blueshift in that of the ν_1 vibrational mode was clearly visible. All these effects were reversible with temperature and, on cooling to 4.5 K, the original absorption profiles were recovered. The main details of the H₂O absorption spectra are summarized in Table I.

As was also observed for the isolated HDO and D₂O monomers, the absorption peaks for all three vibrational modes showed good fits to Lorentzian distributions, indicating that the broadening due to phonon-coupling is homogeneous. A calculation of the area under each peak at different temperatures based on these fits found it to be nearly constant,

TABLE I. Principal features of the absorption spectrum of the H₂O/N₂ system. Here T (K) refers to the substrate temperature; A refers to a peak's amplitude at temperature T normalized against its amplitude at 4.5 K; ν (cm⁻¹) refers to the wavenumber; Δ (cm⁻¹) refers to the transition linewidth (FWHM) obtained from a Lorentzian fit of the optical line shape; $\delta\omega$ (cm⁻¹) refers to the matrix frequency shift relative to the gas phase transition frequency.

T	ν_1				ν_2				ν_3			
	A	ν	Δ	$\delta\omega$	A	ν	Δ	$\delta\omega$	A	ν	Δ	$\delta\omega$
4.5	1.00	3634.9	0.3	-22.2	1.00	1597.0	0.3	2.2	1.00	3727.5	1.2	-28.5
10	0.65	3634.9	0.5	-22.2	0.75	1597.1	0.5	2.3	0.86	3727.5	1.2	-28.5
15	0.38	3634.9	0.7	-22.1	0.56	1597.3	0.8	2.6	0.70	3727.5	1.5	-28.4
20	0.28	3634.9	1.1	-22.1	0.37	1597.6	1.0	2.8	0.63	3727.5	1.9	-28.5
25	0.18	3635.0	1.4	-22.0	0.22	1597.9	1.6	3.1	0.50	3727.3	2.3	-28.6
30	0.11	3635.1	2.0	-22.0	0.16	1598.6	2.4	3.8	0.38	3727.3	2.8	-28.7

meaning that the matrix-molecule interaction can be understood as that of an energetically closed system.

B. HDO/N₂ absorption spectra

The temperature dependent behavior of the HDO vibrational modes in isolation was similar to that of its H₂O analogs. As the temperature increased from 4.5 K to 30 K, a reversible decrease in the amplitudes and a proportional broadening of the linewidths of the absorption peaks can be seen in Figure 2. There is also a clear blueshift in the absorption profile of the ν_2 mode and a much smaller blueshift in that of the ν_1 mode. Full details of the HDO absorption spectra are given in Table II.

A distinctive feature of the HDO/N₂ system is the splitting of the ν_2 and ν_1 mode absorption peaks. Although a second absorption peak is not visible in the spectra of the ν_3 modes, a small shoulder at 3682.2 cm⁻¹ is taken to have

the same origin as the peak splittings. As explained by Cousan *et al.*,⁹ these observations are due to the water molecule occupying a trapping site that distorts the C_{2v} symmetry of the H₂O (and D₂O) monomer. An HDO molecule occupying the same site will then have two possible configurations, with each one producing a distinct set of ν_1 , ν_2 , and ν_3 vibrational mode frequencies.

C. D₂O/N₂ absorption spectra

Figure 3 shows that the temperature dependent behavior of the D₂O/N₂ system was closest to that of the H₂O/N₂ system. As the temperature increased from 4.5 K to 30 K, there was the same reversible decrease in the amplitudes of the ν_1 , ν_2 , and ν_3 mode absorption profiles of 92%, 90%, and 68%, respectively, together with a proportional broadening of their linewidths. The changes in the central positions of the D₂O absorption peaks were also in agreement with previous

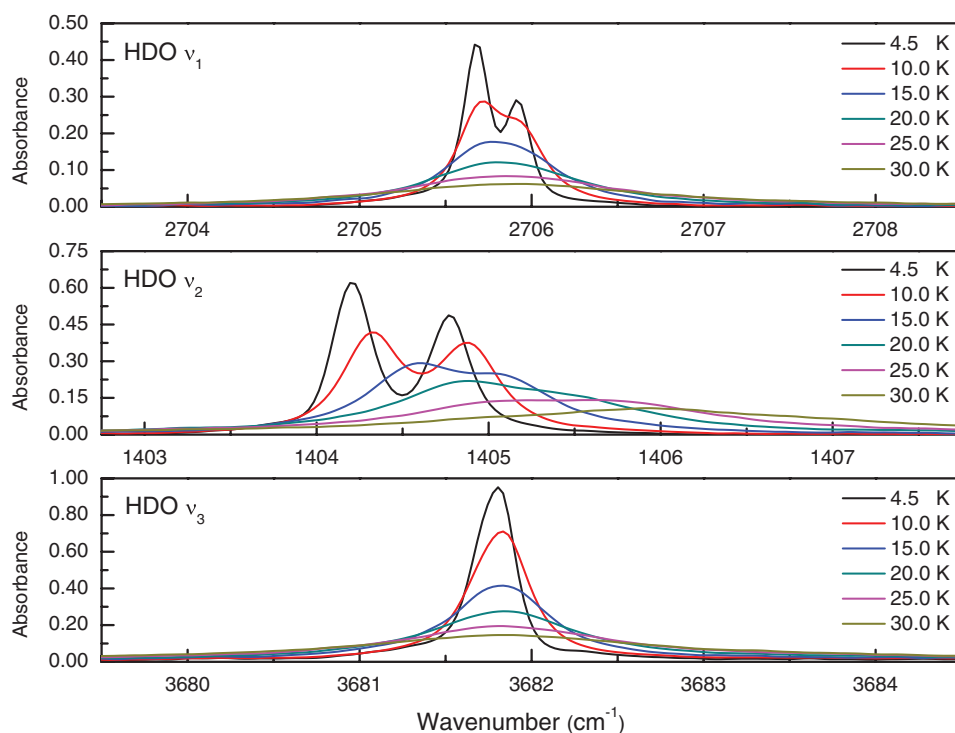


FIG. 2. Temperature dependent behavior of the HDO ν_1 (top), ν_2 (center), and ν_3 (bottom) vibrational bands in the range of 4.5–30 K.

TABLE II. Principal features of the absorption spectrum of the HDO/N₂ system. The units and symbols here are the same as those used in Table I.

T	ν_1				ν_2				ν_3			
	A	ν	Δ	$\delta\omega$	A	ν	Δ	$\delta\omega$	A	ν	Δ	$\delta\omega$
4.5	1.00	2705.7	0.2	-18.0	1.00	1404.2	0.2	0.7	1.00	3681.8	0.3	-25.7
	0.61	2705.9	0.2	-17.8	0.79	1404.8	0.3	1.3				
10	0.53	2705.7	0.3	-18.0	0.67	1404.4	0.4	0.8	0.75	3681.8	0.4	-25.6
	0.39	2705.9	0.3	-17.7	0.60	1404.9	0.4	1.4				
15	0.29	2705.7	0.5	-18.0	0.47	1404.6	0.6	1.1	0.44	3681.8	0.8	-25.6
	0.24	2706.0	0.6	-17.7	0.40	1405.0	0.7	1.5				
20	0.19	2705.7	0.8	-18.0	0.35	1405.9	1.0	1.4	0.29	3681.8	1.3	-25.6
	0.15	2706.0	0.8	-17.6	0.27	1405.4	1.3	1.9				
25	0.20	2705.6	1.0	-18.1	0.22	1405.0	1.5	1.5	0.20	3681.8	2.0	-25.6
	0.09	2706.0	1.2	-17.6	0.22	1405.7	1.7	2.2				
30	0.15	2705.7	1.6	-18.0	0.17	1405.9	2.7 ^a	2.4	0.15	3681.9	3.0	-25.6
	0.10	2706.2	1.9	-17.5	0.17	1405.9	2.7 ^a	2.4				

^aPeaks are very difficult to resolve at high temperature and have therefore been given the same FWHM.

results. The spectrum of the ν_2 mode shows a clear blueshift, while there is almost no shift in the spectrum of the ν_3 mode and only a weak blueshift in the spectrum of the ν_1 mode. Full details of the isolated D₂O absorption spectra are given in Table III.

IV. DISCUSSION

In the general description of the optical excitation of a matrix isolated molecule within a single electronic configuration, relaxation occurs through IR emission, with characteristic lifetime γ_{IR}^{-1} , and parallel vibrational relaxation (VR), with characteristic lifetime γ_{VR}^{-1} . The overall decay rate of the

excited vibrational level is then¹³

$$\tilde{\gamma} = \gamma_{IR} + \gamma_{VR}. \quad (1)$$

The radiative decay rate, γ_{IR} , is temperature independent and is taken here to be negligible compared to the VR rate, γ_{VR} . The explicit temperature dependence of the overall decay rate, $\tilde{\gamma}$, is therefore only determined by the nature of the VR path, i.e., whether it is direct or indirect. An indirect VR process proceeds sequentially: a high frequency vibrational mode is first converted into the one at lowest frequency by intramolecular- and matrix-induced coupling; phonon-coupling subsequently induces VR of the lowest frequency mode by the transfer of energy to matrix phonons. In

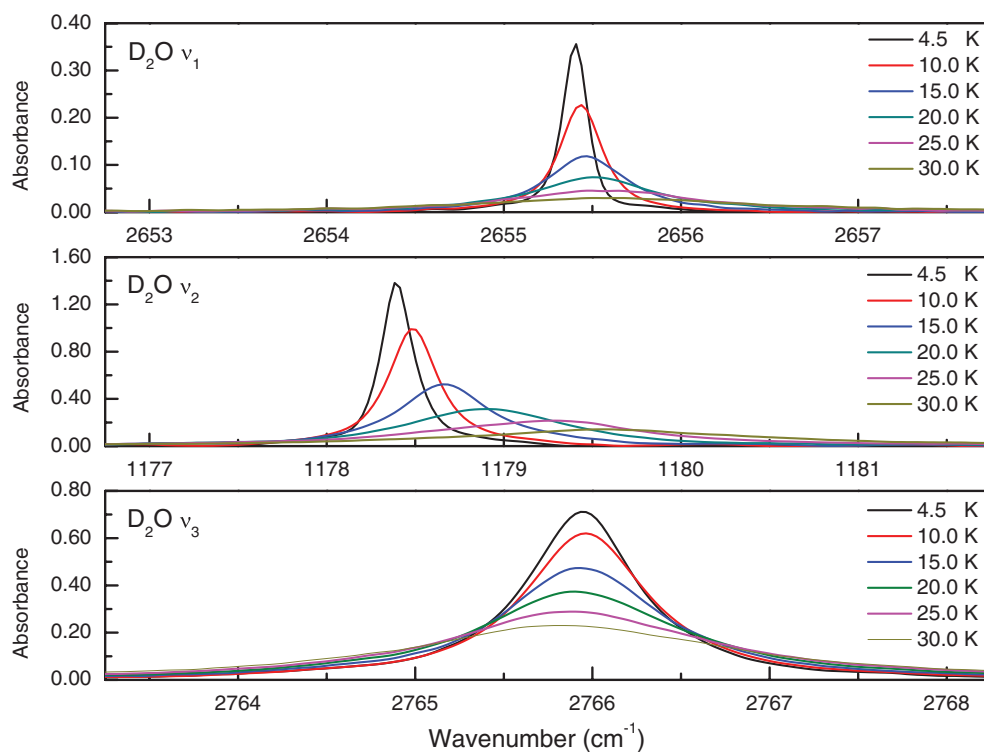


FIG. 3. Temperature dependent behavior of the D₂O ν_1 (top), ν_2 (center), and ν_3 (bottom) vibrational bands in the range of 4.5–30 K.

TABLE III. Principal features of the absorption spectrum of the D₂O/N₂ system. The unit and symbols here are the same as those used in Table I.

T	ν_1				ν_2				ν_3			
	A	ν	Δ	$\delta\omega$	A	ν	Δ	$\delta\omega$	A	ν	Δ	$\delta\omega$
4.5	1.00	2655.4	0.2	-16.2	1.00	1178.4	0.2	0.0	1.00	2766.0	0.7	-21.8
10	0.64	2655.4	0.3	-16.2	0.72	1178.5	0.3	0.1	0.87	2766.0	0.8	-21.8
15	0.33	2655.5	0.5	-16.2	0.38	1178.7	0.6	0.3	0.67	2765.9	1.1	-21.8
20	0.21	2655.5	0.8	-16.2	0.23	1178.9	1.0	0.6	0.53	2765.9	1.3	-21.8
25	0.13	2655.6	1.2	-16.1	0.16	1179.3	1.4	0.9	0.41	2765.9	1.7	-21.8
30	0.08	2655.6	1.9	-16.0	0.10	1179.6	2.0	1.2	0.32	2765.8	2.2	-21.9

a direct VR process, the dissipation of vibrational energy by the excitation of matrix phonons occurs without preliminary decay to other intramolecular modes.

By these definitions, for the isolated H₂O, HDO, D₂O monomers, the VR of the higher frequency ν_1 and ν_3 modes will be indirect with some decay to the lower frequency ν_2 mode. Because of the complexity of the decay processes of the higher energy modes, explicit solutions for their VR rates have not yet been developed. By contrast, the VR of the ν_2 mode is direct and the complications due to intramolecular coupling are absent. In theoretical studies of the lowest energy mode, the molecule is typically treated as a harmonic oscillator weakly coupled to a heat bath representing the matrix. As discussed below, the behavior of this system can then be analyzed by solving the equations of motion arising from various model Hamiltonians.

A. Temperature dependence of the ν_2 vibrational mode

In the present work, the behavior of the ν_2 mode is found to be well-modeled by a Hamiltonian that treats the molecule-matrix coupling as linear in the intramolecular displacements. Solutions to the equations of motion obtained from it have been exposed in detail by Nitzan *et al.*¹² Initial agreement with our experimental observations is seen in the theoretically calculated line shape of the absorption profile, $L(E)$, which at zero temperature ($T = 0$) is a Lorentzian of the form,¹³

$$L(E) \propto \frac{\tilde{\gamma}}{(E - \omega)^2 + \tilde{\gamma}^2}, \quad (2)$$

for which ω is the unperturbed vibrational frequency.

In our analysis of the temperature dependence of Δ for the ν_2 mode, we assume that we are sufficiently close to the above temperature limit that the linewidths of the absorption profiles are equal to the VR decay rate (i.e., $\Delta \simeq \gamma_{VR}$). We therefore make use of the expression derived by Jortner¹⁴ for γ_{VR} in the low temperature regime ($kT/hc < \Omega$),

$$\gamma_{VR}(T)/\gamma_{VR}(0) = 1 + e^{-\beta\Omega} \left(N + \frac{S^2}{N+1} \right), \quad (3)$$

where $\beta = hc/kT$. As defined in Ref. 14, S is the product of the density of phonon states, $\rho_\nu(\Omega_\nu)$, and the square of the molecule-matrix coupling terms, G_ν , integrated over the phonon frequencies, Ω_ν . It is effectively a dimensionless constant measuring the average matrix-molecule coupling strength. The Einstein approximation for the phonon

modes has been invoked, so that the coupled mode has order $N = \omega/\Omega$ and is characterized by an average phonon frequency, $\Omega = \langle \Omega_\nu \rangle$, of the phonon states $\nu = \{1, 2, \dots, N\}$. It should be noted that in the high temperature limit ($kT/hc \gg \Omega$), $\gamma_{VR}(T)/\gamma_{VR}(0)$ is proportional to $1/T$, agreeing qualitatively with the behavior cited for the H₂O/Kr system.⁵

Figure 4 shows the results of a least-squares fit of the linewidths, Δ of Tables I–III, to Equation (3). The gas-phase values were used for ω and the matrix-molecule coupling was assumed to be sufficiently weak that the lowest measured value of Δ could be used as its zero temperature linewidth (i.e., $\Delta(4.5) \simeq \Delta_0$). For reasons not yet fully understood, only the first, lower frequency peak of the HDO/N₂ system could not be adequately fit under these conditions. Nonetheless, the remaining fits gave Ω to be 40 ± 4 cm⁻¹, 36 ± 3 cm⁻¹, and 33 ± 4 cm⁻¹, for isolated H₂O, HDO, and D₂O, respectively. These values show good agreement with each other as would be expected for isotopologs of water isolated in the same matrix. They also show a further consistency in being on the order of the Debye frequency of solid N₂ (69 cm⁻¹).

The least accurate fit was obtained for the HDO/N₂ system, whose relatively high χ^2 value of 2.0 reflects the difficulty in resolving the linewidths of its two peaks. For the H₂O/N₂ system, however, a comparable χ^2 value of 1.5 is attributed to the weakness of the approximation for the zero

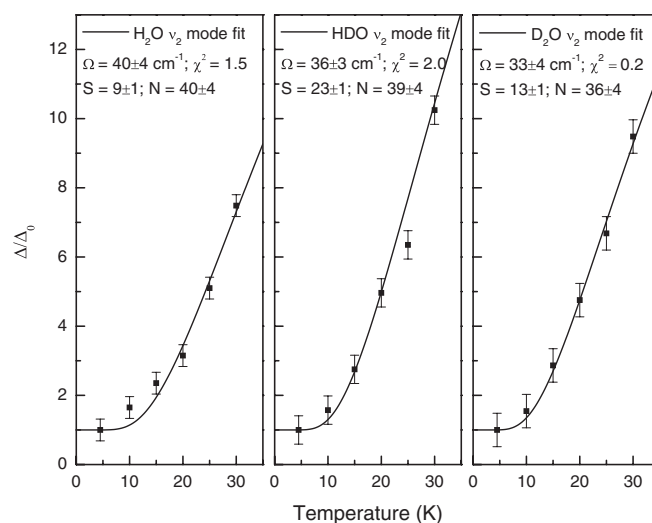


FIG. 4. Least-square fits of the temperature-dependent linewidths, Δ , for the ν_2 mode of matrix isolated H₂O (left), HDO (center), and D₂O (right). Only the second, higher frequency peak for the HDO/N₂ system has been plotted.

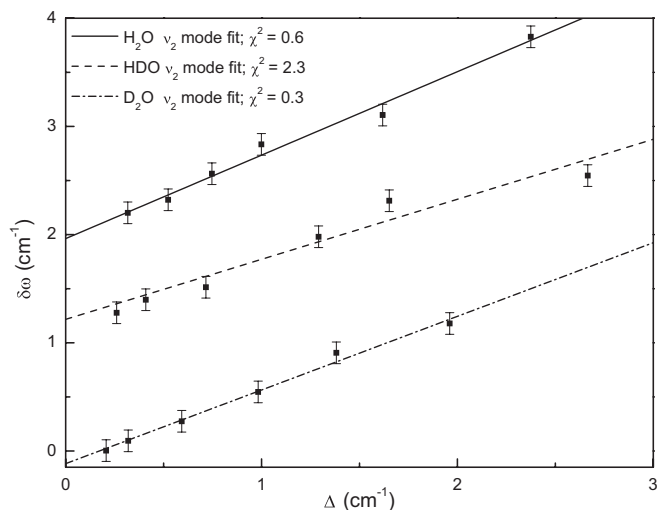


FIG. 5. Least-square fits of the matrix shifts, $\delta\omega$, for the ν_2 mode of matrix isolated H_2O (top), HDO (center), and D_2O (bottom). To accord with Figure 4, only the second, higher frequency peak for the HDO/N_2 system has been plotted.

temperature linewidth in this case, which results in an underestimate of the coupling constant S . Assuming a stronger matrix-molecule coupling for the isolated H_2O monomer would imply that the linewidth is more sensitive to temperature (i.e., $\Delta(4.5) > \Delta_0$), satisfactorily explaining why the observed low temperature linewidths are higher than the theoretical values given by the weak coupling approximation. Conversely, the excellence of the fit for the $\text{D}_2\text{O}/\text{N}_2$ system ($\chi^2 = 0.2$) is attributed to weak matrix-molecule coupling which makes the approximation for the zero temperature linewidth (i.e., $\Delta(4.5) \simeq \Delta_0$) valid.

Figures 1–3 show that the central frequency of the ν_2 mode absorption profile also has a strong dependence on the temperature of the matrix. The matrix shift, $\delta\omega$, has been defined as the difference between this central frequency and the value of the vibrational frequency of the mode in the gas phase. For all three isomers, the frequency of the ν_2 mode is blueshifted (i.e., $\delta\omega$ increases) as the temperature rises. This behavior is attributed to phonon-coupling and the explicit temperature dependence of $\delta\omega$ can be derived to first order from Refs. 6 and 15 as

$$\delta\omega(T) \propto \gamma_{VR}(T)/(\omega - \Omega). \quad (4)$$

The matrix shift is therefore also expected to be proportional to the linewidth. Figure 5 shows the results of least-squares fits of the values of $\delta\omega$ given in Tables I–III to straight lines. The linearity observed between $\delta\omega$ and Δ for each monomer confirms the common origin of their temperature effects. As in Figure 4, the best fit was obtained for the $\text{D}_2\text{O}/\text{N}_2$ system ($\chi^2 = 0.3$), which can be explained by its weak matrix-molecule coupling. Meanwhile, the relative inaccuracy of the fit for the HDO/N_2 system ($\chi^2 = 2.3$) is again understood as being due to the difficulty of resolving the features of its two absorption peaks.

We invoke a simple conservation of energy argument to explain the behavior of the amplitudes (A) of the ν_2

mode absorption peaks. Integration over these peaks for each monomer finds the area under them to be constant at all temperatures, indicating that the absorption and the decay processes form an energetically closed cycle. For a Lorentzian distribution, this area is expressed in terms of a product of the amplitude and the linewidth (i.e., $A\Delta$). The increase in the decay rate due to more efficient VR at higher temperatures can therefore be equivalently expressed by a larger linewidth or a proportionately smaller amplitude.

B. Temperature dependence of the ν_1 and ν_3 vibrational modes

As discussed earlier, analysis of the ν_1 and ν_3 mode is made difficult by the fact that their VR is indirect. To achieve a qualitative interpretation of their behavior in isolation, we broadly identify the linewidth, Δ , with the VR decay rate, γ_{VR} . (Equation (2), however, shows this approximation to be strictly true only for the ν_2 mode in the low temperature limit.) Although absorption features such as the matrix shifts remain unexplained, the temperature dependent behavior of the linewidths is consistent with the picture of direct and indirect VR for high frequency modes.

In Figure 6, the linewidths, Δ , for the ν_1 , ν_2 , and ν_3 modes for isolated H_2O , HDO , and D_2O have been plotted against temperature. The values of Δ for the ν_1 mode are generally observed to be lower than those for the ν_2 mode. Assuming that Δ is strongly correlated to γ_{VR} , we interpret this result as pointing to the ν_2 mode as the principal gateway for relaxation to the ground state once it has been populated by preliminary decay stages from the ν_1 mode. The presence of these preliminary decay stages should be more obvious at high temperature when the ν_2 mode VR becomes most efficient and they act as a bottleneck in the overall decay process. Thus, at low temperature, values of Δ for the ν_1 mode follow closely those for the ν_2 mode. At temperatures

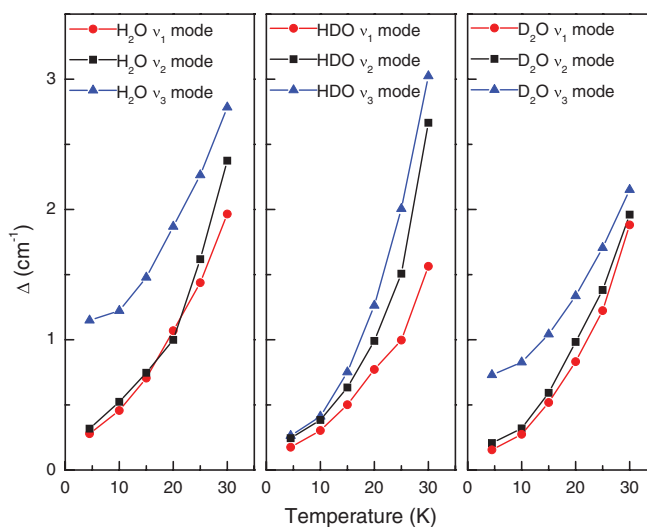


FIG. 6. Plots of the FWHM, Δ , for the ν_1 , ν_2 , and ν_3 modes of matrix isolated H_2O (left), HDO (center), and D_2O (right). Only data for the first, low frequency peaks of the HDO/N_2 system have been plotted, since it is the one most clearly visible for all three modes. For the sake of clarity, error bars have been omitted.

approaching 30 K, however, the plots for H₂O and HDO show that the relaxation rate of the ν_1 mode lags behind that of the ν_2 mode. Due to the weaker matrix-molecule coupling of the D₂O monomer, this effect is likely to be only clearly visible at higher temperatures.

For the isolated H₂O and D₂O monomers, values of Δ for the ν_3 mode are clearly higher than those for the ν_2 mode, supporting the idea that the highest energy mode has the most decay paths available to it. Strong coupling of the ν_3 mode to the N₂ vibron mode (2360 cm⁻¹) would also allow the latter to act as an efficient decay path. In this context, the ν_3 mode of the HDO monomer appears anomalous since its values of Δ are not significantly higher than those of the ν_2 mode at low temperature. A possible explanation is that, despite the availability of other relaxation paths for the ν_3 mode, decay through the ν_2 mode remains the dominant one.

The behavior of the amplitudes of the ν_1 and ν_3 mode absorption peaks can be explained using the same conservation of energy argument above. Assuming indirect VR through the ν_2 mode to be a major decay path, we can expect Δ for the ν_1 and ν_3 modes to be approximately linear with $1/A$. However, the exact relationship between the linewidth and the amplitude of the absorption peak will depend on the nature of the coupling between the ν_2 mode and the ν_1 and ν_3 modes in isolation.

V. CONCLUSIONS

The infrared spectra of H₂O, HDO, and D₂O isolated in solid N₂ have been recorded in the 500–4000 cm⁻¹ range. The vibrational frequencies of the ν_1 , ν_2 , and ν_3 intramolecular modes for each monomer in isolation showed strong temperature dependent behavior. In their corresponding optical profiles, a decrease in the absorption amplitude together with a proportional broadening of the linewidth was observed with increasing temperature. For the ν_1 and ν_3 modes, these observations were qualitatively explained in terms of indirect VR by preliminary decay to the ν_2 mode followed by direct VR via the excitation of matrix phonons. For the lowest frequency ν_2 mode, a quantitative model for direct VR was able to ac-

count for the broadening of the linewidth and the blueshift in the central frequency of the absorption profile with increasing temperature. It also gave average phonon mode frequencies of 40 ± 4 cm⁻¹, 36 ± 3 cm⁻¹, and 33 ± 4 cm⁻¹ for the H₂O/N₂, HDO/N₂, and D₂O/N₂ systems, respectively—on the order of the Debye frequency of solid N₂.

Obvious extensions of this work, such as a study of the temperature dependence of the non-rotational bands of the water monomer isolated in the RGs, are currently being explored. These should provide a deeper understanding of the complex matrix-molecule interactions for the isolated isotopologs of water.

ACKNOWLEDGMENTS

The authors thank Professor A. Engdahl and Professor B. Nelander for useful correspondence and the referee for his constructive comments, all of which were considered in preparing the final version of this paper. It has been jointly supported by the National Science Foundation of China (NSFC) (Grant Nos. 21225314 and 11150110457), the NKBRFSF (Grant No. 2010CB923300), and the FRFCU. R. Lambo gratefully acknowledges support from the Chinese Academy of Sciences.

¹X. Michaut, A.-M. Vasserot, and L. Abouaf-Marguin, *Vib. Spectrosc.* **34**, 83 (2004).

²M. E. Fajardo, S. Tam, and M. E. DeRose, *J. Mol. Struct.* **695–696**, 111 (2004).

³A. J. Tursi and E. R. Nixon, *J. Chem. Phys.* **52**, 1521 (1970).

⁴D. P. Strommen, D. M. Gruen, and R. L. McBeth, *J. Chem. Phys.* **58**, 4028 (1973).

⁵A. Engdahl and B. Nelander, *J. Mol. Struct.* **193**, 101 (1989).

⁶A. Nitzan and S. Silbey, *J. Chem. Phys.* **60**, 4070 (1974).

⁷L. Wan, L. Wu, A.-W. Liu, and S.-M. Hu, *J. Mol. Spectrosc.* **257**, 217 (2009).

⁸J. P. Perchard, *Chem. Phys.* **266**, 109 (2001).

⁹S. Coussan, P. Roubin, and J. P. Perchard, *Chem. Phys.* **324**, 527 (2006).

¹⁰L. Fredin, B. Nelander, and G. Ribbegård, *J. Chem. Phys.* **66**, 4073 (1977).

¹¹M. V. Thiel, E. D. Becker, and G. Pimentel, *J. Chem. Phys.* **27**, 486 (1957).

¹²M. J. Ondrechen, A. Nitzan, and M. A. Ratner, *Chem. Phys.* **16**, 49 (1976).

¹³A. Nitzan and J. Jortner, *Mol. Phys.* **25**, 713 (1973).

¹⁴J. Jortner, *Mol. Phys.* **32**, 379 (1976).

¹⁵A. Nitzan, S. Mukamel, and J. Jortner, *J. Chem. Phys.* **60**, 3929 (1974).